

Determination of minor-actinides fission cross sections by means of the surrogate reaction method

B. Jurado^{1,a}, G. Kessedjian¹, M. Aiche¹, G. Barreau¹, A. Bidaud¹, S. Czajkowski¹, D. Dassié¹, B. Haas¹, L. Mathieu¹, B. Osmanov¹, L. Audouin², N. Capellán², L. Tassan-Got², J.N. Wilson², E. Berthoumieux³, F. Gunsing³, Ch. Theisen³, O. Serot⁴, E. Bauge⁵, I. Ahmad⁶, J.P. Greene⁶, and R.V.F. Janssens⁶

¹ CENBG, Univ. Bordeaux I, CNRS/IN2P3, Le Haut Vigneau, BP. 120, 33175 Gradignan, France

² IPN, Univ. Paris-Sud, CNRS/IN2P3, 91405 Orsay, France

³ CEA Saclay, DSM/DAPNIA/SPhN, 91191 Gif-sur-Yvette Cedex, France

⁴ CEA Cadarache, DEN/DER/SPRC/LEPh, Bât. 230, 13108 Saint-Paul-lez-Durance, France

⁵ CEA, SPN, BP. 12, 91680 Bruyères-le-Châtel, France

⁶ Physics Division, Argonne National Laboratory, 9700 S. Cass Avenue, IL 60439, USA

Abstract. The surrogate reaction method has been used to determine neutron-induced fission cross sections for the short-lived minor actinides $^{242,243}\text{Cm}$ and ^{241}Am . These cross sections are highly relevant for the design of fast reactors capable of incinerating minor actinides. Our results for the fission cross section of ^{242}Cm extend up to the onset of second-chance fission. None of the existing neutron-induced fission data for ^{242}Cm go as high in neutron energy. The latest direct neutron-induced measurement for the ^{243}Cm fission cross section is questioned by our results since there exist differences of more than 60% in the 0.7 to 7 MeV neutron energy range.

1 Introduction

Minor actinides (mainly Np, Am and Cm isotopes) are produced by successive neutron captures, alpha and beta decays starting from ^{238}U in the current U-Pu cycle. These nuclei represent one of the most harmful types of nuclear waste as they are strong neutron and alpha emitters with specific activities, in some cases, on the order of 10^9 Bq/ μg . At present, two different strategic approaches are proposed for minor actinides waste disposal: direct disposal without any reprocessing and spent fuel reprocessing with the aim of optimising the extraction of minor actinides and to incinerate them subsequently. Incineration results in the transmutation of minor actinides into less radiotoxic or short-lived species obtained by neutron-induced fission reactions. The reliable design of reactors for incineration requires an accurate knowledge of minor actinides cross sections in a fast neutron flux. However, in the case of the Cm isotopes, the available data are rather scarce. For instance, the only available data for ^{242}Cm are the cross section measurements for fission induced by neutrons with energies of 0.1–1.4 MeV performed by Vorotnikov et al. in 1984 [1]; no data are available for other decay channels such as $^{242}\text{Cm}(n, \gamma)$, $^{242}\text{Cm}(n, n')$, $^{242}\text{Cm}(n, 2n)$, etc. The reason for this lack of data is the short half-life of ^{242}Cm (163 days) which makes it very difficult to produce and to manipulate targets of this isotope. The experimental technique we present here allows to overcome these difficulties. This indirect method, which is usually called the surrogate method, was developed in the 70's by Cramer and Britt [2]. It consists in measuring the decay probability of a compound nucleus (e.g., fission or radiative capture) produced via an alternative (surrogate) reaction, e.g., a few-nucleon transfer reaction. The chosen surrogate reaction is

such that the resulting nucleus has the same mass A and charge Z as the compound nucleus that would be formed if a neutron would be directly absorbed by the minor actinide. The neutron-induced fission cross section is then deduced from the product of the measured fission probability and the compound nucleus cross section for the neutron-induced reaction obtained from optical model calculations [3]. The surrogate method relies on the validity of the Weisskopf-Ewing limit in which the fission probability is independent of the spin and parity of the compound nucleus. The conditions under which the Weisskopf-Ewing limit applies have been investigated in refs. [4–7]. It was stated in ref. [6] that this limit holds when the excitation energy is high enough for the decay widths to be dominated by the statistical level density and when the angular momentum of the compound nucleus is not much larger than the spin-cutoff parameter of the level density distribution, which, for the actinide region, is around $6\text{--}7 \hbar$. Our group has already applied this technique to the measurement of the neutron-induced fission [8] and capture [9] cross sections of ^{233}Pa via the transfer reaction $^{232}\text{Th}(^3\text{He}, p)^{234}\text{Pa}$. ^{233}Pa plays a fundamental role in the Th/U cycle, but due to its short half-life of 27 days, the available data were rather inaccurate. In the present contribution we will concentrate on a recent experiment where we have applied the surrogate reaction method to determine the neutron-induced fission cross sections of $^{242,243}\text{Cm}$ and ^{241}Am .

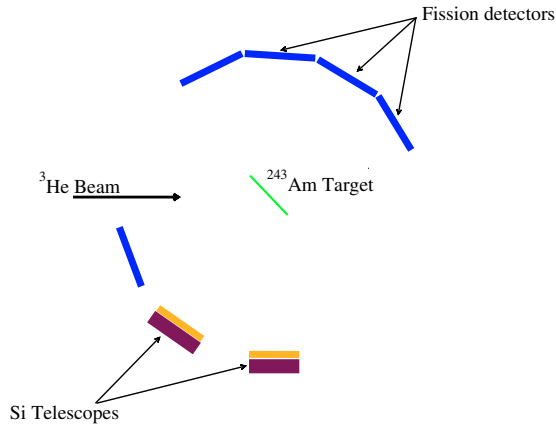
2 Experiment

In this experiment, the access to neutron-rich Cm isotopes via few-nucleon transfer reactions with a light projectile such as ^3He implied the use of a ^{243}Am target. Two targets of approximately $106 \mu\text{g}/\text{cm}^2$ were prepared at the Argonne National Laboratory. Each target was deposited on a 75

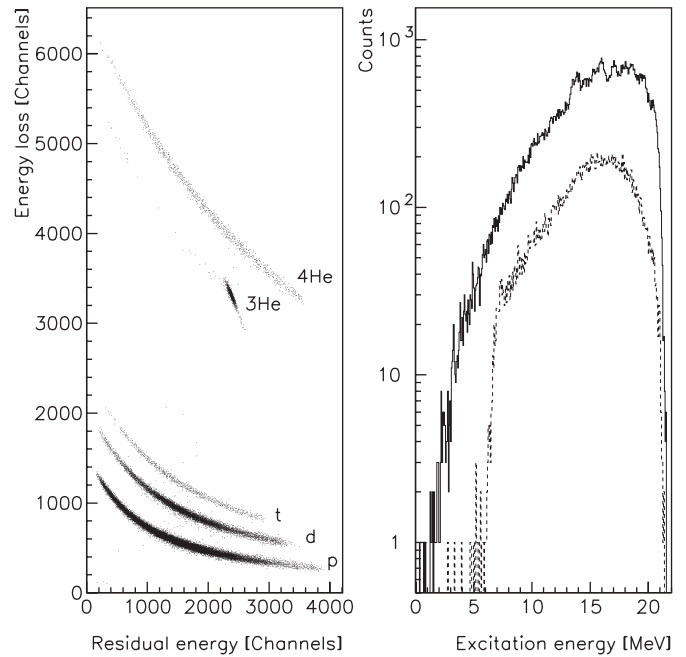
^a Presenting author, e-mail: jurado@cenbg.in2p3.fr

Table 1. Transfer channels investigated in the reaction ${}^3\text{He}+{}^{243}\text{Am}$ and the corresponding neutron-induced fission reactions.

Transfer channel	Neutron-induced reaction
${}^{243}\text{Am}({}^3\text{He}, d){}^{244}\text{Cm}$	${}^{243}\text{Cm}(n, f)$
${}^{243}\text{Am}({}^3\text{He}, t){}^{243}\text{Cm}$	${}^{242}\text{Cm}(n, f)$
${}^{243}\text{Am}({}^3\text{He}, \alpha){}^{242}\text{Am}$	${}^{241}\text{Am}(n, f)$

**Fig. 1.** Top view of the experimental set-up for fission probability measurements of compound nuclei formed via transfer reactions.

$\mu\text{g}/\text{cm}^2$ carbon backing. The ${}^3\text{He}$ beam at 24 and 30 MeV was provided by the Tandem accelerator at the IPN Orsay. The ${}^3\text{He}$ -induced transfer reactions on the ${}^{243}\text{Am}$ target lead to the production of various heavy residues. Table 1 lists the different transfer channels we considered in the present experiment and the corresponding neutron-induced reactions that the surrogate method allows to “reconstruct”. Table 1 illustrates the advantage of using transfer reactions with respect to the standard direct method: the simultaneous access to several transfer channels allows one to determine neutron-induced fission cross sections of various nuclei from just one projectile-target combination. Moreover, since there are two particles in the outgoing reaction channel, the excitation energy of the heavy nucleus E^* follows a broad probability distribution. The compound nucleus excitation energy can be translated into a neutron energy E_n via the relation $E^* = B_n + \frac{A-1}{A}E_n$, where A and B_n are the mass and the neutron binding energy of the compound nucleus, respectively. Therefore, with fixed beam energy, the surrogate method allows the determination of cross sections as a function of neutron energy. The detection set-up used to determine the fission probability of the different compound nuclei formed after a transfer reaction is displayed in figure 1. Two sets of two Si telescopes placed at 90 and 130 degrees with respect to the beam axis served to identify the light charged particles emitted. If the corresponding heavy residue undergoes fission, one of the fission fragments is detected in coincidence with the light particle by means of a fission-fragment multi-detector. This multi-detector was designed to achieve a large efficiency for fission fragment angular distribution measurements. It

**Fig. 2.** Left: Energy loss versus residual energy in one of the Si telescopes. Right: Number of tritons detected in the Si detector located at 130 degrees as a function of the excitation energy of ${}^{243}\text{Cm}$. The full line represents the total number of tritons and the dashed line the tritons detected in coincidence with fission events.

consisted of 15 photovoltaic cells distributed among 5 units, each unit composed of 3 cells placed vertically one above the other. Four units were placed in the forward direction with an angular coverage from 14 to 125 degrees. The fifth unit was positioned at 180 degrees from the foremost unit. In this way, the fission fragments hitting the foremost unit were detected in coincidence with their complementary fragment in one of the cells of the fifth unit. The determination of the kinetic energies of the two fragments of a given fission event allows to infer the fission fragment mass distribution. The fifth unit also serves to add a point at backward angles to the measured angular distribution. More details on the experimental set-up can be found in ref. [8]. The Si telescopes allowed identification of the light charged particles and determination of their kinematics parameters (energy and angle). With this information and the related Q-values, we could determine the excitation energy E^* of the corresponding compound nuclei. The left part of figure 2 shows the energy loss versus the residual energy measured in one of the telescopes. The typical hyperbolas corresponding to the different light charged particles can be easily distinguished. By selecting one type of light particle, for example tritons t , we can construct the spectrum represented by the solid line on the right of figure 2, the so-called “singles” spectrum. This spectrum represents the number of tritons, i.e., the number of ${}^{243}\text{Cm}$ nuclei, N_{sing} , as a function of their excitation energy. The broad peaks at the highest excitation energies stem from transfer reactions on the carbon backing and on ${}^{16}\text{O}$ impurities in the target. The background generated by reactions on the carbon support was measured separately. In this way, we could subtract from the singles spectrum the events arising from reactions on the carbon backing.

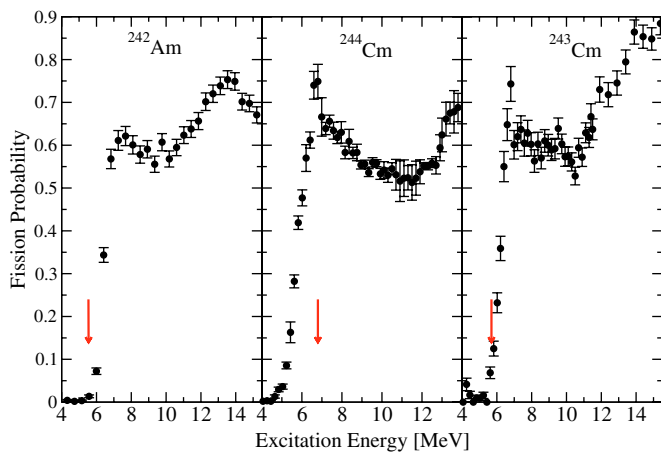


Fig. 3. Preliminary fission probabilities as a function of excitation energy. The arrows indicate the neutron binding energy of the fissioning nucleus.

The remaining singles spectrum has been extrapolated under the ^{16}O peaks, introducing an additional source of uncertainty. If we now select the tritons detected in coincidence with a fission event, we obtain the spectrum represented by the dashed line in the right part of figure 2 which represents the number of ^{243}Cm nuclei that have undergone fission, N_{coin} . For each excitation energy bin we can then determine the ratio between the fission events spectrum (dashed line) and the compound nucleus spectrum (full line). This ratio, corrected for the fission detector efficiency $\text{Eff}(E^*)$, gives the fission probability of ^{243}Cm as a function of the excitation energy: $P_f(E^*) = \frac{N_{\text{coin}}(E^*)}{N_{\text{sing}}(E^*) \cdot \text{Eff}(E^*)}$. The geometrical efficiency of the fission detector is approximately 47%. This efficiency has been calculated with a Monte Carlo simulation that reproduces the experimental efficiency obtained with a ^{252}Cf source. However, for fission induced by neutrons or light charged particles, the fission-fragment angular distributions can be forward peaked. This anisotropy depends on the angular momentum of the system undergoing fission. Therefore, we should actually use an effective detection efficiency that includes not only the geometry of the fission detectors, but also the fragment angular distribution effects. The arrangement of our fission detectors allows to measure the angular distribution anisotropy; with this information and the Monte Carlo simulation it is possible to calculate the effective efficiency. However, the effect of the angular anisotropy on the detector efficiency has not yet been determined; thus, our data have only been corrected for the geometrical efficiency. Nevertheless, as shown in [8] the angular distribution effect is estimated to be of only few %.

3 Results

We have analysed the deuteron, triton and alpha channels which correspond to the fission probabilities of $^{244,243}\text{Cm}$ and ^{242}Am , respectively. The preliminary results are shown in figure 3. Error bars in these spectra represent statistical errors as well as uncertainties due to the subtraction of the contaminant peaks. ^{243}Cm being a fissile nucleus, the neutron binding energy B_n of the compound nucleus ^{244}Cm is higher

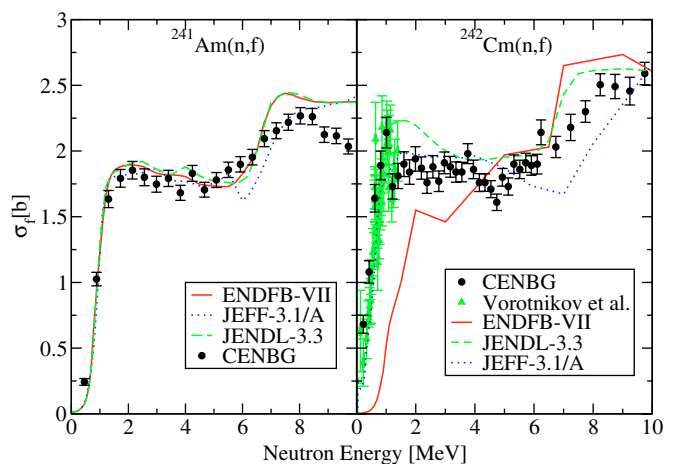


Fig. 4. Preliminary fission cross sections as a function of neutron energy in comparison with the available data and the evaluations.

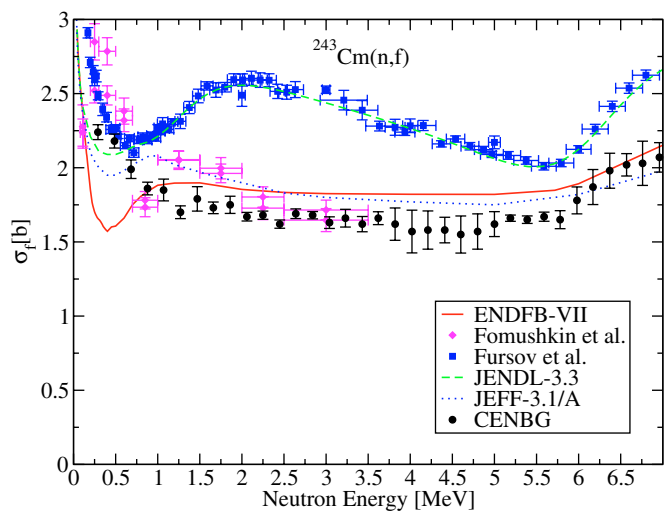


Fig. 5. Preliminary fission cross section as a function of neutron energy in comparison with the available data and the evaluations.

than its fission barrier. Therefore, neutron-induced fission of this nucleus does not allow to explore the fission threshold. As shown in figure 3, the transfer reaction used makes the fission threshold of ^{244}Cm accessible. The preliminary neutron-induced fission cross sections are illustrated in figures 4 and 5. They have been obtained by multiplying the experimental fission probability by the corresponding calculated compound nucleus cross section [3]. The error associated with the compound nucleus cross section of $\sim 5\%$ has not yet been included in the results. As shown in the left panel of figure 4, from the fission threshold up to around 5 MeV the $^{241}\text{Am}(n,f)$ cross section is in very good agreement with all the evaluations, beyond 5 MeV it is not possible to say which evaluation reproduces our data best. The right part of figure 4 shows our results for the $^{242}\text{Cm}(n,f)$ in comparison with the data by Vorotnikov et al. [1]. There is an excellent agreement between both sets of data. For neutron energies larger than 1.4 MeV, no other experimental data exist. This presumably explains the important discrepancies between the various international libraries. JENDL and JEFF present the best overall agreement with our data. The remarkable agreement found at the

lowest neutron energies between our data and the neutron-induced measurements suggests that the spin-parity distributions populated through the transfer reactions used are similar to the ones populated through neutron absorption. The case of the $^{243}\text{Cm}(n,f)$ cross section deserves special attention and is, therefore, plotted separately in figure 5. Our results are compared with the most recent measurements by Fomushkin et al. [10] and by Fursov et al. [11]. At the lowest neutron energies the agreement between the three measurements is rather satisfactory. Beyond 0.7 MeV our data follow fairly well those of Fomushkin [10], but they clearly deviate from the results of Fursov [11]. The biggest discrepancy is found around 2 MeV and amounts to a $\sim 60\%$ difference. Concerning the libraries, in contrast to JENDL, which closely follows Fursov's data, ENDF and JEFF are in rather good agreement with our results. One may wonder whether this discrepancy may be an indication that the angular momentum induced by the nucleon transfer (^3He , d) is much larger than the one induced by neutron absorption and, thus, the Weisskopf-Ewing limit is not applicable in this specific case. However, ref. [6] shows that this effect should lead to an overestimation of the fission cross section. On the other hand, Fursov's cross section in the 1 to 6 MeV energy range is considerably higher than the experimental cross sections of neighbouring fissile isotopes such as ^{245}Cm [12, 13] and ^{247}Cm [11] which are systematically below 2 barns. Moreover, under the reasonable assumption that the neutron inelastic scattering cross section of ^{243}Cm ranges from 1 to 1.5 barn at 2 MeV neutron energy, the value of the fission cross section of 2.6 barn obtained by Fursov et al. at 2 MeV would give a total compound cross section (we neglect the capture contribution to the total compound cross section) varying from 3.6 to 4.1 barns, which is considerably larger than the 3 barns predicted by the optical model calculations of ref. [3]. All these arguments suggest that Fursov's results overpredict the $^{243}\text{Cm}(n,f)$ cross section at neutron energies larger than 0.7 MeV.

Besides the relevance of these fission data for minor actinides incineration, the comparison of the measured cross sections with model calculations will enable the determination of fundamental fission parameters such as fission barrier heights and curvatures as well as the investigation of low-lying transition states which are not well known for these short-lived nuclei. In addition, once the model parameters are fixed, cross sections that are hardly measurable, such as (n,γ) and (n,n') , can be predicted.

4 Conclusions and perspectives

The design of nuclear reactors capable of incinerating minor actinides requires a good knowledge of neutron-induced cross sections of Cm and Am isotopes. However, the enormous specific activity of these nuclei considerably complicates the direct measurement of these cross sections. We have presented the first results of a recent experiment to determine the neutron-induced fission cross sections of $^{242,243}\text{Cm}$ and ^{241}Am using the surrogate reaction technique. The deduced $^{241}\text{Am}(n,f)$ and $^{242}\text{Cm}(n,f)$ cross sections are in good agreement with the

available data obtained via neutron-induced reactions. The present data constitute the first measurement of the $^{242}\text{Cm}(n,f)$ cross section above 1.4 MeV. Our results for the $^{243}\text{Cm}(n,f)$ cross section are clearly below the latest results of Fursov et al. beyond 0.7 MeV [11]. The final cross section data will be compared to model calculations based on the statistical model. This comparison will allow one to determine several fundamental fission parameters and predict neutron-induced cross sections such as (n,γ) and (n,n') , which are otherwise difficult to measure. Apart from the fission cross sections, fission-fragment mass distributions are also very important for the operation/safety of a reactor as they are strongly related to the reactor neutron balance and to the radioactivity of the used fuel. Indeed, fission fragments radioactivity has a direct consequence on the decay heat inside the reactor and some fission products like Xe, Sm, Eu and Gd isotopes can act as neutron poisons in nuclear reactors. Finally, the mass distributions of the fission products are also of interest for determining the yield of delayed neutrons, which play a vital role in the controllability of reactors. The existing experimental data on fission-fragment yields of minor actinides are very deficient. Our experimental set-up will allow to determine the fission fragment mass distributions of the compound nuclei investigated in this work and to study their evolution with neutron energy. The energy-dependent fission fragments yields represent, as well a strong added value to fundamental nuclear physics as they will lead to a better understanding of the physics of fission and, in particular, of the role of shell effects on the fission process.

We thank the tandem accelerator staff and the target laboratory of the IPN Orsay for their great support during the experiment. This work was partly supported by the CNRS programme PACEN/GEDEPEON, the Conseil Régional d'Aquitaine, the US Department of Energy, Office of Nuclear Physics, under contract DE-AC02-06CH11357, and by the EURATOM project "TRANSMA" (FP6-044556). The authors are also indebted for the use of ^{243}Am to the Office of Basic Energy Sciences, US Department of Energy, through the transplutonium element production facilities at Oak Ridge National Laboratory.

References

1. P.E. Vorotnikov et al., *Yadernaya Fizika* **40**, 1141 (1984).
2. J.D. Cramer, H.C. Britt, *Nucl. Sci. Eng.* **41**, 177 (1970).
3. E. Bauge (private communication).
4. W. Younes, H.C. Britt, *Phys. Rev. C* **67**, 024610 (2003).
5. W. Younes, H.C. Britt, *Phys. Rev. C* **68**, 034610 (2003).
6. J.E. Escher et al., *Phys. Rev. C* **74** 054601 (2006).
7. J.E. Escher et al. (these proceedings).
8. M. Petit et al., *Nucl. Phys. A* **735**, 345 (2004).
9. S. Boyer et al., *Nucl. Phys. A* **775**, 175 (2006).
10. E.F. Fomushkin et al., *Atomnaya Energiya* **69**, 258 (1990).
11. B.I. Fursov et al., *Conf. Nucl. Data for Sci. and Techn., Trieste, 1997*, Vol. 1, p. 488.
12. E.F. Fomushkin et al., *Atomnaya Energiya* **63**, 242 (1987).
13. R.M. White et al., *Conf. Nucl. Data for Sci. and Techn., Antwerp, 1982*, p. 218.